

See discussions, stats, and author profiles for this publication at: <https://www.researchgate.net/publication/8250924>

# Calorimetric and structural investigation of the interaction of lysozyme and bovine serum albumin with poly(ethylene oxide) and its copolymers

ARTICLE *in* COLLOIDS AND SURFACES B: BIOINTERFACES · NOVEMBER 2004

Impact Factor: 4.15 · DOI: 10.1016/j.colsurfb.2004.08.004 · Source: PubMed

---

CITATIONS

26

---

READS

47

4 AUTHORS, INCLUDING:



**Iris L Torriani**

University of Campinas

158 PUBLICATIONS 2,230 CITATIONS

SEE PROFILE



**Watson Loh**

University of Campinas

105 PUBLICATIONS 2,238 CITATIONS

SEE PROFILE

# Calorimetric and structural investigation of the interaction of lysozyme and bovine serum albumin with poly(ethylene oxide) and its copolymers

Nara L. Almeida<sup>a</sup>, Cristiano L.P. Oliveira<sup>b,c</sup>, Iris L. Torriani<sup>b,c</sup>, Watson Loh<sup>a,\*</sup>

<sup>a</sup> Instituto de Química, Universidade Estadual de Campinas, Caixa Postal 6154, 13083-970 Campinas, SP, Brazil

<sup>b</sup> Instituto de Física Gleb Wataghin, Universidade Estadual de Campinas, 13083-970 Campinas, SP, Brazil

<sup>c</sup> Laboratório Nacional de Luz Síncrotron, Campinas, SP, Brazil

Received 30 July 2004; received in revised form 17 August 2004; accepted 17 August 2004

## Abstract

This work reports investigations aiming at verifying the occurrence of specific interactions between lysozyme or bovine serum albumin (BSA) and poly(ethylene oxide) and its copolymers with poly(propylene oxide). Thermal stability of these proteins, followed by means of high sensitivity DSC, was found to be mostly unaffected by the presence of these polymers. Chromatographic experiments (reverse-phase HPLC and size exclusion chromatography) did not reveal any sign of specific interaction for these mixtures, either. Isothermal titration calorimetry revealed an increase in enthalpy for the mixtures, represented by a positive enthalpy of transfer for these proteins from buffer to polymer solutions. Moreover, SAXS analyses confirmed that at ambient temperatures these polymers do not affect lysozyme structure. In summary, no evidence is found to support earlier suggestions that some kind of complex could be formed between these proteins and poly(ethylene oxide) or its copolymers, but the present results suggest the occurrence of entropically driven hydrophobic effects.

© 2004 Elsevier B.V. All rights reserved.

**Keywords:** Protein denaturation; Calorimetry; Bovine serum albumin; Lysozyme; Poly(ethylene oxide)

## 1. Introduction

Poly(ethylene oxide) and its copolymers are widely used in biomedical formulations both for their high solubility in water and biocompatibility [1]. One of their most prominent applications is in preventing protein adsorption onto surfaces, improving their biocompatibility or onto particles leading to increased in vivo half-lives [2]. Similar reasons led to the development of what is now called “pegylation” [3], i.e., chemical attachment of small poly(ethylene oxides), also known as poly(ethylene glycols), PEG, to proteins aiming at producing active bioconjugates, with increased half-lives.

The nature of the physico-chemical interaction between PEO and proteins is still an open issue. The ability to avoid protein adsorption over PEO-covered surfaces has been associated with steric hindrance, directly related to PEO chain

conformation [4,5] so that the higher its molar mass, the less effective the van der Waals attraction forces between protein and surface and, hence, the smaller the extent of adsorption [5]. However, attractive forces were detected between PEO and proteins in some particular cases, namely: at low surface coverage with grafted high molar mass [6] and at high compressive loads [7,8] or by decreased PEO hydration at higher temperatures [8], in a surface force measurement apparatus. There are also reports on complex formation in solutions of PEO and human serum albumin, based on evidences from chromatographic [9,10] and scattering measurements [10].

Recently, a series of reports from Topchieva and coworkers, presented evidence for non-covalent complexes formed between alpha-chymotrypsin and PEO [11,12] or ethylene oxide/propylene oxide copolymers [13]. In some cases, complex formation was increased by centrifuging their mixture, what was ascribed to reduced PEO solvation under higher pressure [13]. One of the evidences presented for complex formation included a slight increase in protein thermal

\* Corresponding author. Tel.: +55 19 3788 3148; fax: +55 19 3788 3023.  
E-mail address: [wloh@iqm.unicamp.br](mailto:wloh@iqm.unicamp.br) (W. Loh).

stability upon polymer addition, as revealed by DSC measurements, and different elution behavior in affinity chromatography. On the other hand, a previous investigation on protein (urease and interleukin 2) mixtures with F127 EO/PO copolymer reported no change of protein thermal stability [14].

These earlier somewhat contradictory findings, and the relevance of this still elusive phenomenon, prompted us to carry out the present investigation. In this work, we report analyses on mixtures between two proteins, BSA and lysozyme, with PEO of different molar masses, and EO/PO triblock copolymers of varied composition. This investigation was conducted using calorimetric techniques to investigate polymer effect on protein thermal stability (by high sensitivity DSC) and the energetics of possible protein-polymer interactions (by isothermal titration calorimetry). Moreover, the formation of polymer-protein complexes was also explored with chromatographic measurements and, for lysozyme, by structural investigation through small angle X-ray scattering (SAXS) analyses.

These proteins were chosen for possessing different sizes and isoelectric points: 17 kDa and  $pI = 11$  for lysozyme and 66 kDa and  $pI = 4.8$  for BSA, and for the existence of previous studies on their thermal denaturation. PEO with molar masses ranging from 400 to 100 000  $\text{g mol}^{-1}$  were used. This molar mass range encompasses the transition from a polyglycol to polyether character, ascribed at ca. 2000  $\text{g mol}^{-1}$  [15], above which hydroxyl contributions were found out to no longer affect PEO solution behavior. The copolymers used in the present investigation have their chemical structures depicted in Table 1. Some of them, F108, P105 and P103, represent samples for which the hydrophobic middle group contains similar number of PO units, with increasing number of hydrophilic EO units. For other series of copolymers, F38, F68 and F108, the ratio of EO/PO units is constant, but their molar mass increases. With this choice of copolymers, we wish to probe the effect of their hydrophobicity (or of their aggregates) and of their molar mass on possible interactions with lysozyme and BSA.

The use of EO–PO–EO block copolymers provides another interesting feature besides the possibility of varying the copolymer hydrophobicity. Owing to different aqueous solubility of hydrophilic EO units and hydrophobic PO units, these copolymers display well-documented self-assembling

in solution [16–19]. Their aggregation may be directed either by increasing concentration, occurring above a critical micelle concentration (c.m.c.), or by increasing temperature, with threshold at a critical micelle temperature (c.m.t.). Hence, interaction of proteins may be investigated in the presence of non-aggregated polymer (called unimers), or with their aggregates.

Understanding possible interaction between proteins and PEO or its copolymers is of additional importance for the increasing use of these polymers in protein separation processes based on aqueous two-phase systems [20,21].

## 2. Experimental

### 2.1. Materials

Hen egg white lysozyme and bovine serum albumin (BSA) were purchased from Sigma, USA. Polymers and copolymers used are described in Table 1. Mono and dibasic sodium phosphate and acetic acid were purchased from Labsynth, Brazil. Potassium chloride was purchased from Merck, Brazil and sodium acetate, from Nuclear, Brazil. Water of Milli Q grade was used throughout. Buffer at pH 7.0 was prepared at concentration of 0.01  $\text{mol L}^{-1}$ , with ionic strength adjusted to 0.05  $\text{mol L}^{-1}$  with NaCl. At pH 4, acetate buffer had a concentration of 0.01  $\text{mol L}^{-1}$ .

### 2.2. High sensitivity DSC (HSDSC) measurements

Thermal denaturation of proteins was monitored with a high sensitivity differential scanning calorimeter, model VP-DSC, from MicroCal Inc. Thermograms were obtained between 20 and 90 °C, at a scan rate of 60 °C  $\text{h}^{-1}$ . Both proteins were analyzed at concentrations of 5  $\text{mg mL}^{-1}$ . Some test experiments performed at lower concentrations (1  $\text{mg mL}^{-1}$ ) produced essentially the same curves, ruling out significant contributions from concentration effects. All results are averages of, at least, three independent measurements.

The calorimetric data were analyzed by using the software Origin 5.0, MicroCal Inc., according to the methodology recommended by IUPAC [22]. The parameters obtained from this analysis were: temperature at which maximum heat

Table 1  
Description of polymers used in this study

Polymer	Source	$M^a$ ( $\text{g mol}^{-1}$ )	EO units <sup>a</sup>	PO units <sup>a</sup>	c.m.t. <sup>b</sup> (2.5% solution) (°C)
PEO	Sigma (USA)	3350	76	–	–
PEO	Fluka (Germany)	35000	795	–	–
PEO	Aldrich (USA)	300000	6818	–	–
F 38	ICI Surf., UK	4800	2 × 44	17	60
F 68	ICI Surf., UK	8350	2 × 76	30	43
F 108	ICI Surf., UK	14000	2 × 127	50	23
P 105	ICI Surf., UK	6500	2 × 37	58	18
P 103	ICI Surf., UK	4950	2 × 17	62	16

<sup>a</sup> Average values calculated from their nominal molar mass.

<sup>b</sup> Critical micelle temperatures, determined as the onset temperature of the aggregation peaks from DSC curves.

exchange occurs,  $T_m$ , the width of the peak at half-height,  $\Delta T_{1/2}$ , and the area under the peak, which represents the enthalpy of transition for reversible processes.

### 2.3. Isothermal titration calorimetry (ITC)

Titration experiments were conducted in a Thermometric 2277 calorimeter, previously calibrated by the electrical substitution method, which has been confirmed by chemical calibration using the dilution of aqueous propanol [23]. Experiments were performed by adding six aliquots of 30  $\mu\text{L}$  of a 100  $\text{mg mL}^{-1}$  protein solution to an ampule containing 2.5 mL of a polymer solution (at 2.5 wt.%). The energy associated with the interaction between protein and polymer is calculated by discounting the heats of dilution of protein and polymer, which were determined by the titration of a protein solution into buffer and of buffer into polymer solutions, respectively. Results were expressed as enthalpy of transfer, by dividing the heat exchanged both by the number of moles of protein and amino acid residues added.

### 2.4. Size exclusion chromatography (SEC)

These chromatographic experiments were performed in a Waters 650 liquid instrument, using a G 75 Sephadex column. 200  $\mu\text{L}$  of a 20  $\text{mg mL}^{-1}$  protein solution at pH 7.0 was injected using the buffer as eluent at a 1  $\text{mL min}^{-1}$  flow rate. Experiments in the presence of polymer were performed the same way, with solutions containing 6 wt.% polymer. Compounds were detected with a UV-vis Waters 490E detector at 280 nm for the proteins and, for PEO, the colorimetric method proposed by Nag et al. [24] was used.

### 2.5. Reverse-phase HPLC

These experiments were conducted with an HPLC Waters 510 instrument using a photodiode array detector Waters 991. Samples were prepared in phosphate buffer, at pH 7.0, containing 5  $\text{mg mL}^{-1}$  protein and, for some experiments, 2.5 wt.% polymer. The elution program started with pure 1% trifluoroacetic acid, linearly increasing the acetonitrile content until finishing with pure acetonitrile after 60 min.

### 2.6. Sample treatment at high pressures

For some experiments, samples were previously exposed to high pressures by either centrifugation or exposure to high hydrostatic pressure. Centrifugation was performed in a Beckman Microfuge, operating at 13 000 rpm, with a radius of 55.8 mm (equivalent to 10 600 g), for 30 min. For exposure to higher hydrostatic pressures, an apparatus similar to the one described by Paladini and Weber [25] was used. Samples were left under pressure of 25 000 MPa (ca. 250 000 atm), for 30 min at room temperature.

### 2.7. Small angle X-ray scattering measurements

SAXS analyses were performed at the SAXS beam-line of the Brazilian Synchrotron Light Laboratory, Campinas, Brazil. The wavelength selected for the experiments was  $\lambda = 1.49 \text{ \AA}$  and the distance between the sample and detector was 745 mm. The samples were exposed in a 1.5 mm capillary tube in a thermally controlled sample holder directly connected to the evacuated beam path. These experiments were performed with lysozyme samples at 10  $\text{mg mL}^{-1}$  and pH 7.0 (phosphate buffer). For samples containing polymers, their concentration was 2.5 wt.%. Some samples were submitted to high pressures (as described above), ca. 30–60 min before the SAXS measurements.

Data treatment was performed using the software package TRATID [26]. Usual corrections for detector homogeneity, incident beam intensity, sample absorption and blank subtraction were included in this routine. The output of this software provides the corrected intensities and error values necessary for data analysis. Since the protein + polymer + buffer samples are ternary systems, to extract the scattering of the pure protein from the total intensity curve, the scattering from a blank sample consisting of polymer + buffer was subtracted from the protein + polymer + buffer scattering curves. The resulting scattering intensity was compared with the intensity obtained for the pure protein in a separate experiment with a protein + buffer sample.

### 2.8. Theoretical details of the SAXS analysis

From the SAXS theory we know that the intensity of a system composed of particles in solution, with polydispersity in the form factors can be expressed as

$$I(q) = \left[ \sum_i N_i (\Delta\rho_i)^2 V_i^2 P_i(q) \right] S_{1,2,\dots,i}(q) \quad (1)$$

where  $N_i$ ,  $\Delta\rho_i$ ,  $V_i$  and  $P_i(q)$  are the number of particles, the electron density contrast, the particle volume and the particle form factor of each type of scattering particle. The factor  $S_{1,2,\dots,i}$  represents the possible particle–particle interaction that can be expressed for example by the Percus–Yevick equation or Monte Carlo simulations [27]. If we have very low particle concentration, we can assume as a first approximation no particle interaction,  $S_{1,2,\dots,i} \approx 1$ . As a result, the total intensity can be expressed as the sum of the intensity scattered by each individual phase component.

$$I(q) = \sum_i I_i(q) \quad (2)$$

Since the intensity can then be described by a Fourier transform of the pair distance distribution function  $p(r)$  according

to Eq. (3):

$$p(r) = \frac{1}{2\pi^2} \int_0^\infty r q I(q) \sin(rq) dq \quad (3)$$

the  $p(r)$  function for the multiple phase system can be written as a sum of each component phase contribution.

$$p(r) = \sum_i p_i(r) \quad (4)$$

Since this function provides information on the shape of the scattering particles and their maximum dimension, there is a possibility of extracting this information for the protein from the three-component system and comparing it with the parameters obtained for the pure protein in buffer solution. This was one of the procedures adopted in this work trying to detect possible structural changes and/or interactions.

Another type of analysis can be made using the so-called Kratky plots ( $I(q)q^2$ ), whose behavior is related to the globular nature of the proteins, reflecting their degree of folding and changes on their compactness. For a system with compact shape and sharp phase boundaries, this plot shows a well-defined curve with an initial upward portion followed by a descending curve. On the other hand, the curve for a polymer in an extended or random coil conformation shows a characteristic plateau and rises at higher angles [28].

All curve fittings and calculations in this work were performed using the GNOM software package [29].

### 3. Results

Results from thermal denaturation of BSA at pH 7 and 4, in absence and presence of the different copolymers, are summarized in Tables 2 and 3, respectively. For all of the studied concentrations, the copolymers P103, P105 and F108 are al-

Table 2  
Experimental data for thermal denaturation of BSA at pH 7

System	$T_m$ (°C)	$\Delta T_{1/2}$ (°C)	Area (kJ mol <sup>-1</sup> )
Pure protein	60.0 ± 0.4	6.0 ± 0.2	350 ± 50
0.25% of polymer			
F 38	56.3 ± 0.1	6.1 ± 0.8	430 ± 350
F 68	57.7 ± 0.1	5.8 ± 0.5	130 ± 25
F 108	56.1 ± 0.1	6.1 ± 0.6	260 ± 90
P 103	56.0 ± 0.2	7.1 ± 0.8	360 ± 50
P 105	56.7 ± 0.1	5.3 ± 0.8	180 ± 70
PEO 3350	56.6 ± 0.1	5.9 ± 0.6	350 ± 50
PEO 35000	56.0 ± 0.2	6.4 ± 0.5	350 ± 80
PEO 100000	56.8 ± 0.4	5.7 ± 0.6	210 ± 33
2.5% of polymer			
F 38	56.6 ± 0.1	6.1 ± 0.4	480 ± 50
F 108	56.7 ± 0.1	5.8 ± 0.6	150 ± 20
P 105	56.7 ± 0.4	6.8 ± 0.2	370 ± 70
PEO 3350	57.1 ± 0.3	5.8 ± 0.9	270 ± 110
PEO 35000	57.0 ± 0.1	6.2 ± 0.5	270 ± 54
PEO 100000	55.6 ± 0.2	7.3 ± 0.7	400 ± 190

Table 3

Experimental data for thermal denaturation of BSA at pH 4.0 in solutions with 2.5 wt.% of polymer

System	$T_m^1$ (°C)	$T_m^2$ (°C)	Area <sup>1</sup> (kJ mol <sup>-1</sup> )	Area <sup>2</sup> (kJ mol <sup>-1</sup> )
Pure protein	45.3 ± 0.1	67.5 ± 0.2	303 ± 3	237 ± 3
F 108 <sup>a</sup>	47.8 ± 0.1	66.7 ± 0.1	230 ± 2	238 ± 2
P 103 <sup>a</sup>	52.3 ± 0.3	60.6 ± 0.2	514 ± 22	601 ± 21
P 105 <sup>a</sup>	47.1 ± 3.6	68 ± 3	579 ± 39	698 ± 38
PEO 3350	48.0 ± 0.1	65.9 ± 0.1	340 ± 3	322 ± 3
PEO 35000	48.5 ± 0.1	64.9 ± 0.1	378 ± 2	318 ± 3
PEO 100000	49.5 ± 0.1	66.5 ± 0.2	319 ± 3	254 ± 3

These thermograms showed two peaks (see text) and 1 and 2 refer to first and second peaks.

<sup>a</sup> Solutions where copolymer aggregates are present.

ready aggregated at temperatures lower than the denaturation temperature of both proteins, hence, the proteins denature in the presence of copolymer micelles. For F38 and F68, in 2.5% solution, copolymer aggregates form within the denaturation temperature range. At the low concentration level, 0.25%, these two copolymers do not form aggregates within the studied temperature range. The values of  $T_m$  and  $\Delta T_{1/2}$  should reflect changes in the protein thermal stability, as measured by the maximum in the  $C_p$  versus temperature curve and by the width at half-height of the transition peak. At pH 7 (Table 2), the presence of all polymers, at the two concentrations investigated (0.25 and 2.5 wt.%), caused a decrease of ca. 4–5 °C in  $T_m$ , without significant changes in the peak width. At pH 4, BSA thermal denaturation is known to proceed with two distinct endothermic peaks [30,31] as shown in Fig. 1, ascribed to the melting of independent domains of the protein due to formation of a crevice in its structure. In the present investigation, these denaturation curves were deconvoluted using the Microcal Origin software. The separated transitions hence allowed determination of transition

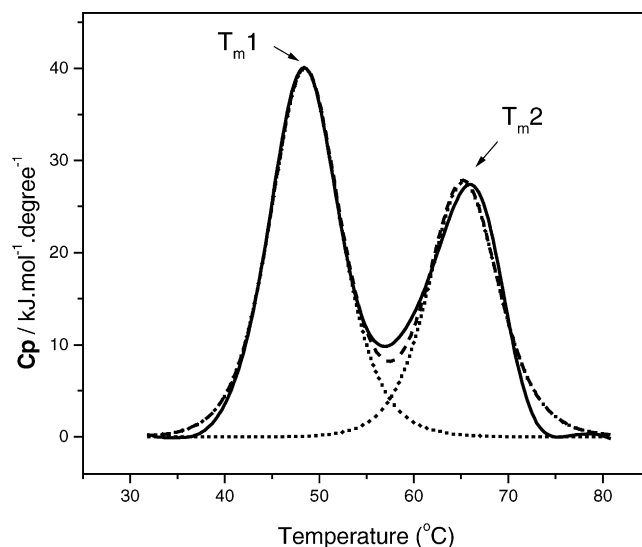


Fig. 1. DSC curve for thermal denaturation of BSA at pH 4. The solid line corresponds to the calorimetric data, dashed and dotted lines are produced by deconvolution.



parameters. Data presented in Table 3 show that the first denaturation peak is shifted to slightly higher temperatures, opposite to what is observed for the second peak. In any case, these changes comprise just a few degrees.

The energy involved in the transition is also listed in Tables 2 and 3. It is clear that values for the energy of transition show poor reproducibility at pH 7, while a much better reproducibility is observed for values associated with BSA denaturation at pH 4. This poor reproducibility may be ascribed to the irreversible nature of this transition, as pointed out by Michnik [30]. It is interesting to notice that  $T_m$  and the curve width do not change so much, in agreement with indications that these difference in the energies of transition are due to different amounts of protein undergoing denaturation. No attempt is made to interpret these energies for experiments at pH 7, but, at pH 4, it is possible to detect a significant increase in the energy involved in the transition ascribed to BSA denaturation in the presence of P103 and P105 when compared with those of pure BSA and of BSA with the more hydrophilic copolymer F108 or PEO of different molar masses.

Data for the denaturation of lysozyme were determined only at pH 7, since its isoelectric point is quite high, and the equipment used did not allow experiments above it. These data, shown in Table 4, reveal no significant changes in lysozyme protein stability, as measured by  $T_m$ , in the presence of any of the polymers investigated. Lysozyme thermal denaturation is assumed to be a reversible two-step process, as we confirmed by analyses of the denaturation thermograms, which is followed by an irreversible aggregation of the denaturated protein [32–34]. Hence, the energy involved in the transition may be considered as an enthalpy change, which is confirmed by the good reproducibility of the data shown in Table 4. Analysis of these data points out to a significant increase in the enthalpy of transition when lysozyme is in the presence of the micelle forming copolymers F38 and P105 (for these copolymers, DSC curves show that micelle formation occurs at temperatures below the denaturation temperature), while no significant variation is observed upon addition of PEO. The aggregation of denaturated lysozyme can be visually followed due to turbidity increase. We observed that the point at which turbidity appears is shifted to higher temperatures, from ca. 80 to above 85 °C, when lysozyme is heated at 1 °C min<sup>-1</sup> in the presence of micelles of these two copolymers, indicating their effect on protein aggregation.

Table 4  
Experimental data for thermal denaturation of lysozyme at pH 7 with 2.5 wt.% of polymer

System	$T_m$ (°C)	$\Delta_t H$ (kJ mol <sup>-1</sup> )
Pure protein	73.2 ± 0.2	420 ± 30
PEO 3350	72.8 ± 0.1	440 ± 50
PEO 35000	72.7 ± 0.6	500 ± 64
F 38 <sup>a</sup>	71.8 ± 0.4	842 ± 140
P 105 <sup>a</sup>	73.4 ± 0.3	607 ± 57

<sup>a</sup> Solutions where copolymer aggregates are present.

Table 5  
Experimental HSDSC data from thermal denaturation of lysozyme and BSA in 2.5 wt.% additive solution

Additives	BSA $T_m$ (°C)	Lysozyme $T_m$ (°C)
Pure protein	60.0	73.0
Ethylene glycol	60.1	73.1
Diethylene glycol	60.1	73.3
Triethylene glycol	60.1	73.1
PEO 400	60.2	–
PEO 1000	60.3	–
PPO 425	59.2	72.9
PPO 1000	59.3	–

Earlier investigations [34] reported the stabilizing effect of some polyols on the thermal denaturation of lysozyme, but at much higher concentrations than the ones used in the present study. To investigate whether similar effects contribute to the data presented in Tables 3 and 4, we have followed thermal denaturation of BSA and lysozyme, at pH 7, in the presence of 2.5 wt.% of some glycols and ethylene oxide and propylene oxide oligomers, but no significant changes in the denaturation temperatures were observed (see data in Table 5).

Another set of experiments to assess protein thermal stability was conducted based on earlier reports by Topchieva and coworkers [11–13], who proposed that the formation of the PEO-protein complexes they reported was associated to pressure increase during centrifugation of these mixtures. Moreover, those authors reported that these complexes were kinetically stable for up to 3 days, after centrifugation was performed. For this reason, mixtures of proteins and polymers were submitted to centrifugation at 10 600 g and, subsequently, analyzed by HSDSC.

These measurements were performed less than 1 h after centrifugation, but no change in  $T_m$  or  $\Delta_t H$  values was observed. In order to study further the effect of high pressure some samples were submitted to high hydrostatic pressures (25 000 MPa, ca. 250 000 atm), for 30 min, at room temperature. After this, DSC curves were obtained and, once again, no difference was observed for any of the parameters related to protein thermal stability with respect to measurements without pressurization.

The possibility of formation of non-covalent complexes between lysozyme, BSA and PEO or EO/PO copolymers

Table 6  
Retention time values (in min) from size exclusion and reverse-phase chromatography

Solution	$t_R$ from SEC	$t_R$ from HPLC
BSA	72.4	40.7
BSA + PEO 3350	73.3	40.7
BSA + PEO 3350 centrifuged	72.2	40.9
BSA + PEO 35000	–	41.5
BSA + PEO 35000 centrifuged	–	41.0
Lysozyme	–	17.4
Lysozyme + PEO 35000	–	17.5
lysozyme + PEO 35000 centrifuged	–	17.1

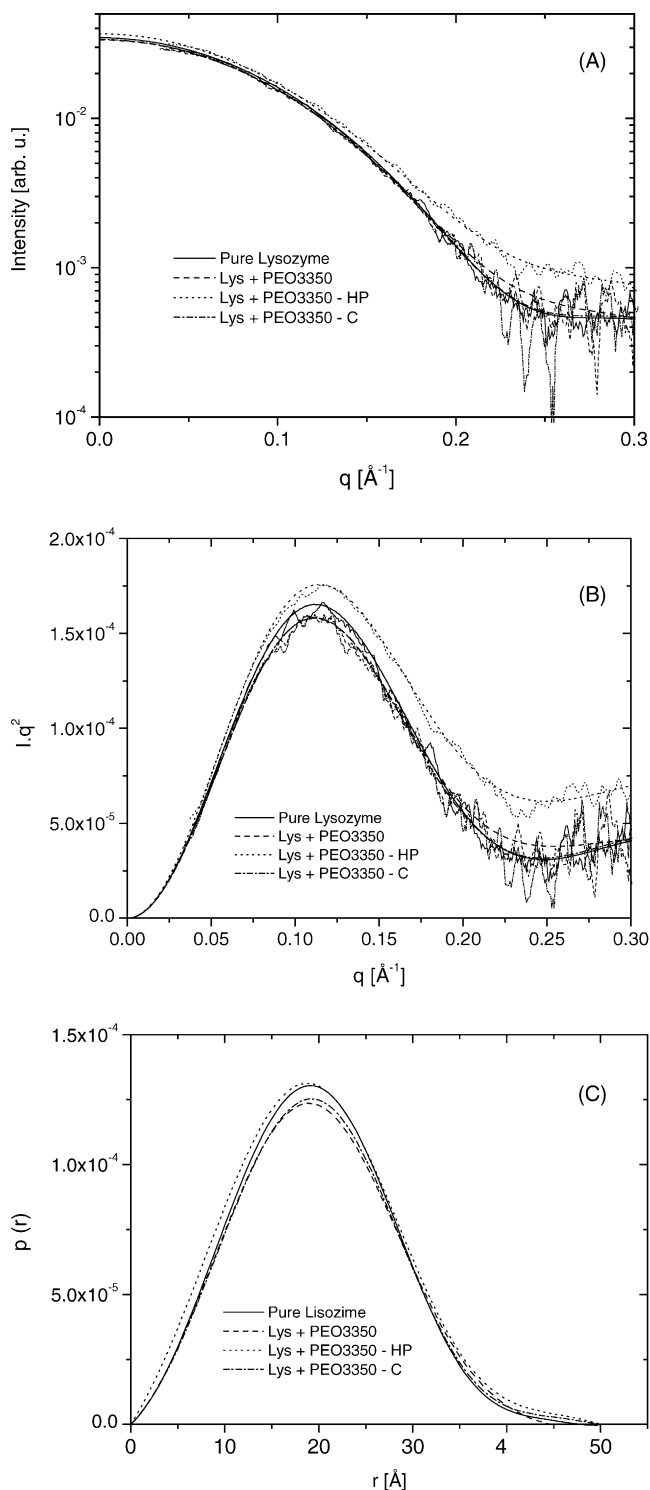


Fig. 2. (A) Corrected SAXS intensity curves, (B) Kratky plots and (C) pair distance distribution functions for the system lysozyme + PEO 3350 under normal conditions, after being subjected to high pressure (HP), and after centrifugation (C). In (A) and (B) each experimental curve is shown superimposed to its corresponding GNOM fit (smooth curve).

was also assessed through chromatographic measurements. Two chromatographic techniques were employed: size exclusion chromatography (SEC) as a means of detecting protein complexation through increase in size, and consequent

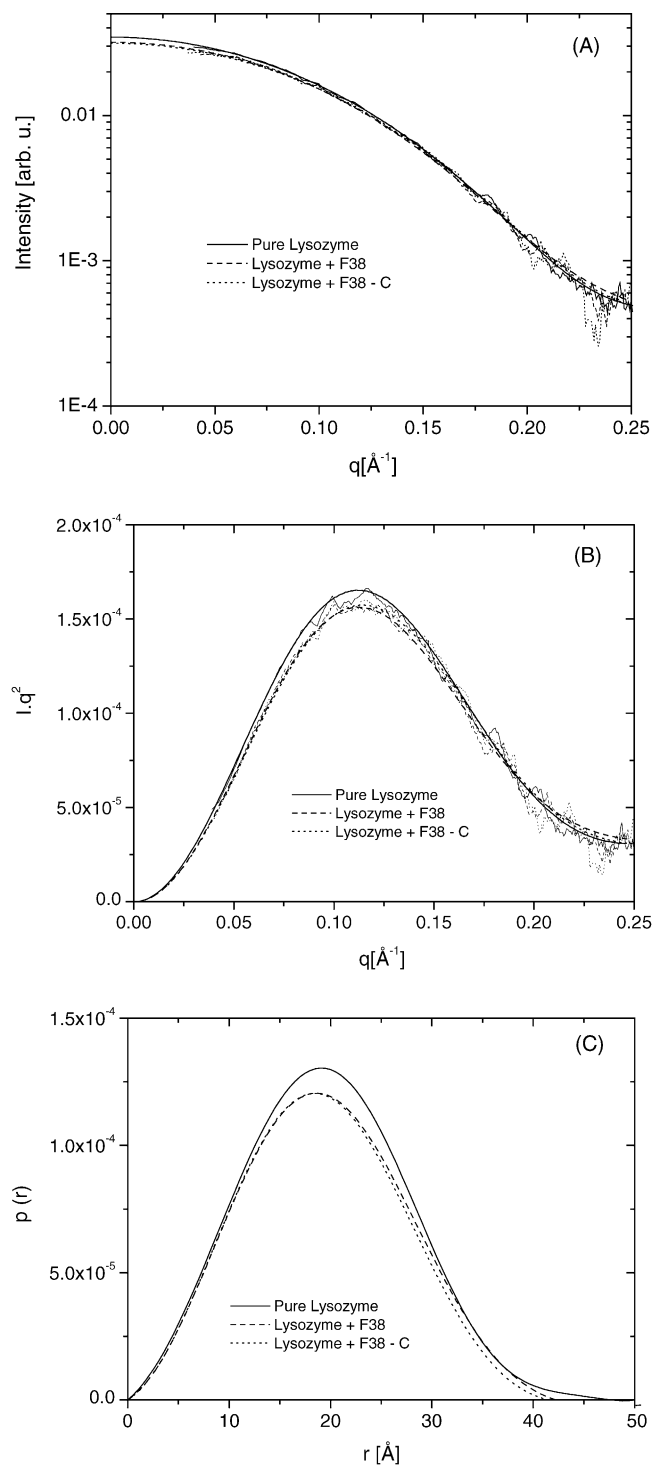


Fig. 3. (A) Corrected SAXS intensity curves, (B) Kratky plots and (C) pair distance distribution functions for the system lysozyme + F38 under normal conditions, after being subjected to centrifugation (C). In (A) and (B) each experimental curve is shown superimposed to its corresponding GNOM fit (smooth curve).

decrease in retention time; and reverse-phase HPLC, by assessing changes in protein solubility on complexation. Results from both techniques are shown in Table 6, revealing that no change in protein retention time is observed by either

mixing with PEO and copolymers or by centrifugation of these mixtures.

A more detailed structural investigation was performed by SAXS analyses of lysozyme mixtures with PEO and block-copolymers. Figs. 2(a–c), 3(a–c) and 4(a–c) show the corrected SAXS intensity curves as well as the corresponding Kratky plots and  $p(r)$  functions for the three systems studied. The intensity functions for the lysozyme + PEO 3350 system under normal conditions, after being subjected to high pressure and after centrifugation (Fig. 2a), present similar behavior. For the three conditions studied, the average particle radius of gyration calculated is practically the same as that of the pure protein in solution, within the experimental error (see Table 7) and in good agreement with the values reported in the literature [35]. A slight difference is noted for the protein + polymer sample subjected to high pressure. In this case there is a contribution to the total scattering, probably due to a change in the degree of coiling of the polymer under pressure in the presence of the protein. The Kratky plot for this same sample (Fig. 2b) shows an increase in the curve  $I(q)q^2$  versus  $q$  for larger values of  $q$ , typical of a system containing random coil structures. The  $p(r)$  functions, shown in Fig. 2c, indicate that the overall shape of the protein is not affected by the presence of the polymer in the solution. We could only note a small change in the shape of the curve for the sample subjected to high pressure, with an increase in the number of short distances due to the increase of the scattering intensity at higher angles.

Fig. 3(a–c) shows the results for the mixture lysozyme + F38. For these samples there are no specific changes in protein conformation. As can be seen in Fig. 3a, the intensity functions are almost coincident with the pure protein curve and, as shown in Table 7, the values of the average radius of gyration calculated for the scattering particles are also very close to that of the pure protein in solution. The Kratky plots (Fig. 3b) all indicate a fairly compact structure, and the  $p(r)$  functions (Fig. 3c) correspond to globular shaped particles, with no significant differences between the pure lysozyme structure in solution and the polymer-protein mixture, even after centrifugation.

Finally, Fig. 4(a–c) shows the results for the system lysozyme + P105 (6500 Da). The scattering intensities show

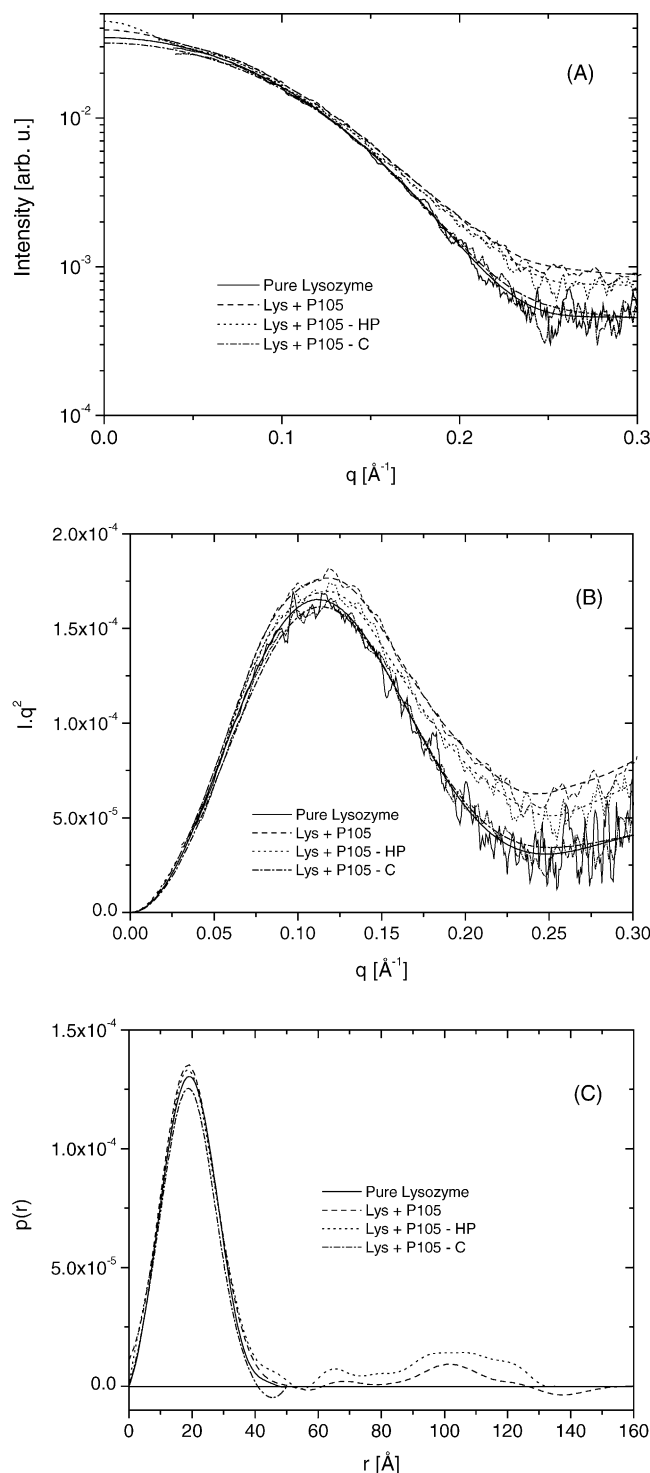


Fig. 4. (A) Corrected SAXS intensity curves, (B) Kratky plots and (C) pair distance distribution functions for the system lysozyme + P105 under normal conditions, after being subjected to high pressure (HP), and after centrifugation (C). In (A) and (B) each experimental curve is shown superimposed to its corresponding GNOM fit (smooth curve).

differences at very low  $q$  values and also at the largest  $q$  values. When the sample is subjected to high pressures, there is an increase in the intensity at low angles (see Fig. 4a), very likely due to residual scattering from polymer micelles not

Table 7  
Changes of radius of gyration of the protein in the presence of the polymers PEO, F38 and P105

Sample	$R_g$ ( $\text{\AA}$ )
Pure Lysozyme	$15.0 \pm 0.3$
(Lysozyme + PEO)	$15.0 \pm 0.3$
(Lysozyme + PEO) – under high pressure	$15.2 \pm 0.5$
(Lysozyme + PEO) – centrifuged	$15.2 \pm 0.4$
(Lysozyme + F38)	$14.6 \pm 0.6$
(Lysozyme + F38) – centrifuged	$14.5 \pm 0.4$
(Lysozyme + P105)	$27 \pm 10$
(Lysozyme + P105) – under high pressure	$33 \pm 9$
(Lysozyme + P105) – centrifuged	$14.3 \pm 0.7$



eliminated after the blank (polymer + solvent under pressure) subtraction. This could be explained assuming that there is a larger population of micelles in the protein + polymer + solvent system because the presence of the protein somehow favors micelle formation. The average particle radius of gyration for this system is much larger than that of the pure protein (see Table 7). This can be attributed to the contribution to  $R_g$  from the much larger polymer micelles present in the system (when particles of various sizes are present, heavy weighting is placed on those with largest sizes). It is also noted that centrifugation of the protein-polymer sample produces a system whose intensity curve is very close to that of the pure protein. This fact is well observed in the  $p(r)$  functions corresponding to pure lysozyme and to centrifuged lysozyme + P105 (Fig. 4c). On the other hand, both lysozyme + P105 in normal conditions and after being subjected to high pressure, both give rise to pair distance distribution functions in which the initial part matches that of the pure protein and a second part extends up to much larger values of  $r$ . This can be interpreted according to Eq. (4) as a result of the contribution of two populations of independent scatterers: the proteins and the polymer micelles. According to this interpretation, the longer distances are due to the polymer micelles (larger than the protein) present in the system. In spite of this fact, the shape of the protein does not change. The  $p(r)$  function corresponding to the polymer micelles presents some oscillations and poor definition due to the low micelle concentration in the sample. This behavior of the  $p(r)$  function would indicate the absence of any interaction between these macromolecules.

The possibility of complex formation between these proteins and polymers was also investigated by using isothermal titration calorimetry. Enthalpy changes associated with the transfer of proteins from buffer to polymers solutions were calculated from the enthalpies of protein dilution in buffer and in polymer solution. As protein is titrated into the polymer solution, polymer in the ampoule is also diluted, giving rise to another enthalpic contribution which has been discounted by measuring the heat of injecting buffer into polymer buffer solution. Heat exchanged during these titrations was within 10 mJ and 1 J, small, but above the equipment sensitivity limit. Only for dilution of BSA in buffer, heat exchanged was too small to be determined, smaller than 200  $\mu$ J per injection. Duplicate experiments were performed for each set of dilutions, with deviations smaller than 10% for BSA and 1% for lysozyme.

Values of enthalpies of transfer were calculated both on the basis of moles of protein and of moles of amino acid residues, as shown in Figs. 5 and 6, providing upper and lower limits to the energy involved in possible interactions.

All values shown in Figs. 5 and 6 reveal that the protein transfer from buffer to polymer solutions is an endothermic process and, as such, no indication of existence of specific interactions between protein and polymers is obtained.

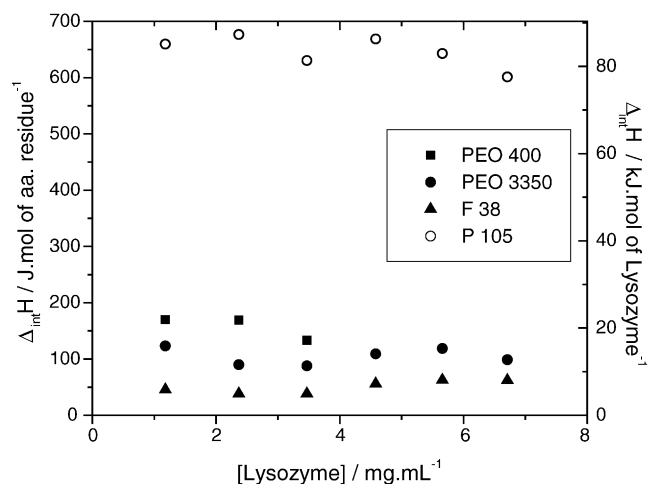


Fig. 5. Enthalpy of transfer of lysozyme from buffer to a polymer solution.

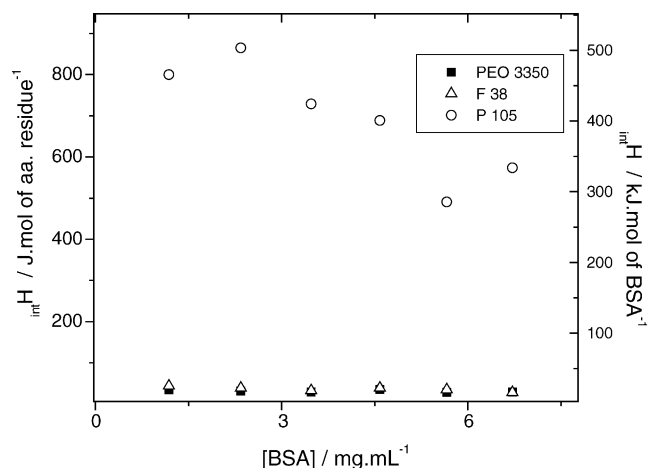


Fig. 6. Enthalpy of transfer of BSA from buffer to a polymer solution.

#### 4. Discussion

Overall, the experiments conducted as part of the present investigation revealed no sign of the occurrence of specific interaction between these two proteins and any of the polymers studied. Reverse-phase HPLC and SEC revealed no alteration of proteins solubility nor size, when in the presence of these polymers, differently from earlier reports of similar investigations [13]. Thermal stability of both BSA and lysozyme was only slightly affected by the presence of PEO or EO/PO block copolymers, with more intense changes observed for BSA at pH 7. In this specific case, these findings point out to some effect of these polymers in stabilizing the denatured state of BSA, similarly to what has been proposed to explain the effect of denaturants like urea [36] and guanidine hydrochloride [37]. It is likely that this effect occurs due to some degree of preferential solvation by these polymers of the protein hydrophobic moieties, exposed upon denaturation.

Determination of enthalpies of transfer for the protein from buffer to polymer solutions support this view, revealing

a positive enthalpy of transfer, which would represent a barrier to any polymer-protein interaction, that has to be overcome by a favorable entropic contribution. A recent report by Farrugia et al. [38], also describes positive enthalpy changes for the mixture of BSA and PEO of two molar masses, in agreement with the present investigation. Similar approach has been applied to the investigation of the interaction between lysozyme and short chain alcohols [39], producing evidence that at low alcohol concentration transfer enthalpies were positive, whereas at higher alcohol content they change sign, a behaviour that has been related to alcohol effects on water structure. In this context, any specific interaction is expected to be favored by enthalpy, hence should be associated with a negative enthalpy of transfer [40].

Therefore, from the present results, any interaction between these proteins and polymers could only occur if entropically controlled, not falling into the category proposed in earlier investigation [13], but more similar to hydrophobic interactions. Additionally, entropy-driven solution processes involving PEO, or its copolymers, aqueous solutions have been recently reported – see for instance [41–44], as associated with the release of polymer hydration molecules, and may also explain the non-specific preferential solvation of denatured BSA by some polymers.

A much larger value for the enthalpy of transfer was determined for solutions where copolymer aggregates are present (P105 and F38), suggesting that native BSA and lysozyme may, somehow, interact with these aggregates in a way to produce a higher extent of dehydration, most likely of the polymer. Interestingly, such an effect does not seem to be pronounced enough to affect these proteins solution properties, which should alter their elution behaviour in either SEC or reverse-phase HPLC, nor their thermal stability. The only change observed to parallel such findings was an increase in the energy associated with the denaturation of lysozyme and BSA (at pH 4), in the presence of copolymer aggregates (see Tables 3 and 4). Presence of polymers may affect the extent of protein–protein interaction, including aggregation processes. If these processes are exothermic, their decrease may cause an increase in the overall observed transition enthalpy, explaining the differences verified in the data listed in Tables 3 and 4. Preliminary investigations on the kinetics of lysozyme aggregation in the presence of P105 aggregates [45] revealed that this temperature-induced process is slowed down by the presence of copolymer aggregates, reinforcing the view that P105 aggregates may interact with hydrophobic moieties, particularly those exposed upon protein denaturation, reducing the extent of protein–protein interaction.

Part of the experiments performed in the present study followed an earlier proposition that PEO-protein interaction may be forced by pressure increase upon centrifugation [12,13]. We tried to repeat the same centrifugation protocol and even exposed mixtures to much higher hydrostatic pressures, with no detectable changes in protein elution behavior, thermal stability and, for lysozyme, SAXS curves. One possible problem with our approach was that samples were ana-

lyzed 30–60 min after being exposed to high pressures, based on the reports that effects associated with this complexation lasted up to 3 days. Such an assumption may not hold for these systems. More investigations should be conducted to verify those earlier reports, especially considering the possibility of conducting the experiments under high pressure, and not after pressure was released. However, the present results, at least, suggest the possibility that those earlier claims of complex formation between hydrophilic polymers and proteins may need to be revised.

## Acknowledgements

Authors gratefully acknowledge the Brazilian Agencies FAPESP, for research grants and for scholarships (to N.L.A and C.L.P.O.), and CNPq, for senior researcher grants (to W.L. and I.L.T.), and the Brazilian Synchrotron Light Laboratory for allocation of beam time that allowed the SAXS measurements. Profs. Carlos F. S. Bonafé and Sergio Marangoni are also thanked for allowing use of their equipments for high pressure and chromatography experiments.

## References

- [1] J.M. Harris, Poly(ethylene glycol) Chemistry – Biotechnical and Biomedical Applications, Plenum Press, New York, 1992.
- [2] Y. Mori, S. Nagaoka, H. Takiuchi, N. Noguchi, H. Tanzawa, Y. Noishiki, Trans. Am. Soc. Artif. Internal. Org. 28 (1982) 459.
- [3] A.T. Abuchowski, N.C. Palczuk, F.F. Davis, J. Biol. Chem. 252 (1977) 3578.
- [4] R.C.L. Wang, H.J. Kreuzer, M. Grunze, J. Phys. Chem. B 101 (1997) 9767.
- [5] P. Harder, M. Grunze, R. Dahint, G.M. Whitesides, P.E. Laibinis, J. Phys. Chem. B 102 (1998) 426.
- [6] E.P.K. Curie, J. Van der Gucht, O.V. Borisov, M.A. Cohen Stuart, Pure Appl. Chem. 71 (1999) 1227.
- [7] S.R. Sheth, D. Leckband, Proc. Natl. Acad. Sci. U.S.A. 94 (1997) 8399.
- [8] N.V. Efremova, S.R. Sheth, D.E. Leckband, Langmuir 17 (2001) 7628.
- [9] D.L. Cocke, H. Wang, J. Chen, Chem. Commun. (1997) 2331.
- [10] S. Azegami, A. Tsuboy, T. Izumi, M. Hirata, P.L. Dublin, B. Wang, E. Kokufuta, Langmuir 15 (1999) 940.
- [11] N.V. Efremova, E.M. Sorokina, B.I. Kurganov, I.N. Topchieva, Biochemistry (Moscow) 63 (1998) 441.
- [12] I.N. Topchieva, E.M. Sorokina, N.V. Efremova, A.L. Ksenofontov, B.I. Kurganov, Bioconjugate Chem. 11 (2000) 22.
- [13] I.N. Topchieva, N.V. Efremova, Y.A.E. Snitko, N.V. Khvorov, Doklady Chem. 339 (1994) 257.
- [14] P.L. Wang, P.C. Johnston, Int. J. Pharm. 96 (1993) 41.
- [15] M. Spitzer, E. Sabadini, W. Loh, J. Braz. Chem. Soc. 13 (2002) 7.
- [16] B. Chu, Langmuir 11 (1995) 414.
- [17] P. Alexandridis, T.A. Hatton, Colloid. Surface A 96 (1995) 1.
- [18] W. Loh, in: A. Hubbard (Ed.), Encyclopedia of Colloid and Surface Science, Marcel Dekker, New York, 2002, p. 802.
- [19] O. Glatter, G. Scherf, K. Schillén, W. Brown, Macromolecules 27 (1994) 6046.
- [20] M. Svensson, F. Joabsson, P. Linse, F. Tjerneld, J. Chromatogr. A 761 (1997) 91.

- [21] A. Nilsson, H.O. Johansson, M. Mannesse, M.R. Egmond, F. Tjerneld, *Biochim. Biophys. Acta-Proteins Proteom.* 1601 (2002) 138.
- [22] H.J. Hinz, F.P. Schwarz, *Pure Appl. Chem.* 73 (2001) 745.
- [23] G. Olofsson, D. Berling, N. Markova, M. Molund, *Thermochim. Acta* 347 (2000) 31.
- [24] A. Nag, G. Mitra, P.C. Ghosh, *Anal. Biochem.* 237 (1996) 224.
- [25] A.A. Paladini, G. Weber, *Rev. Sci. Instrum.* 52 (1981) 419.
- [26] C.L.P. Oliveira, TRAT1D - Computer Program for SAXS Data Treatment, LNL Technical Manual MT01/2003.
- [27] D. Frenkel, B.M. Mulder, *Mol. Phys.* 55 (1985) 1171.
- [28] O. Glatter, O. Kratky, *Small Angle X-ray Scattering*, Academic Press, New York, 1982.
- [29] V. Semenyuk, D.I. Svergun, *J. Appl. Cryst.* 24 (1991) 537.
- [30] A. Michnik, *J. Therm. Anal. Calorim.* 71 (2003) 509.
- [31] M. Yamasaki, H. Yano, K. Aoki, *Int. J. Biol. Macromol.* 12 (1990) 263.
- [32] F.P. Schwarz, *Thermochim. Acta* 147 (1989) 71.
- [33] S. Cinelli, A. De Francesco, G. Onori, A. Paciaroni, *Phys. Chem. Chem. Phys.* 6 (2004) 3591.
- [34] C. Tanford, *J. Mol. Biol.* 73 (1973) 185.
- [35] M. Hirai, S. Arai, H. Iwase, T. Takizawa, *J. Phys. Chem. B* 102 (1997) 1308.
- [36] V. Prakash, C. Loucheux, S. Scheufele, M.J. Gorbunoff, S.N. Timasheff, *Arch. Biochem. Biophys.* 210 (1981) 455.
- [37] C. Tanford, K.C. Aune, *Biochemistry* 9 (1970) 206.
- [38] B. Farruggia, B. Nerl, G. Picó, *J. Chromatogr. B* 798 (2003) 25.
- [39] P. Westh, Y. Koga, *J. Phys. Chem. B* 101 (1997) 5755.
- [40] W. Loh, A.E. Beezer, J.C. Mitchell, *Thermochim. Acta* 255 (1995) 83.
- [41] M. Spitzer, E. Sabadini, W. Loh, *J. Phys. Chem. B* 106 (2002) 12448.
- [42] R.C. da Silva, W. Loh, G. Olofsson, *Thermochim. Acta* 417 (2004) 295.
- [43] L.H.M. da Silva, W. Loh, *J. Phys. Chem. B* 104 (2000) 10069.
- [44] J.R. Lopes, W. Loh, *Langmuir* 14 (1998) 750.
- [45] C.L.P. Oliveira, N.L. de Almeida, W. Loh and I.L. Torriani, unpublished results.